Research Square

Preprints are preliminary reports that have not undergone peer review.
They should not be considered conclusive, used to inform clinical practice,
or referenced by the media as validated information.

Synthesis and Properties of Bombyx Mori Chitosan Nanoascorbate Complexes Based on Oligochitosan and High-molecular-weight Chitosan

Kudrat Kadambayevich Pirniyazov

qudratpirniyazov8875@gmail.com

Институт химии и физики полимеров АН РУз https://orcid.org/0009-0005-7014-7686

Research Article

Keywords: chitosan nanoascorbate from Bombyx mori, polymeric preparative form

Posted Date: August 18th, 2026

DOI: https://doi.org/10.21203/rs.3.rs-10722541/v1

License: This work is licensed under a Creative Commons Attribution 4.0 International License.
Read Full License

Additional Declarations: The authors declare no competing interests.

UDK 595.132:591

SYNTHESIS AND PROPERTIES OF *BOMBYX MORI* CHITOSAN NANOASCORBATE COMPLEXES BASED ON OLIGOCHITOSAN AND HIGH-MOLECULAR-WEIGHT CHITOSAN

K.K. Pirniyazov[*,a,1], S.Sh. Rashidova [b,1]

[1]Institute of Polymer Chemistry and Physics, Academy of Sciences of the Republic of Uzbekistan, 7B A. Qodiriy Street, Tashkent 100128, Uzbekistan**

***Correspondence: qudratpirniyazov8875@gmail.com**

[a]https://orcid.org/0009-0005-7014-7686

[b]https://orcid.org/0000-0003-3104-6004

Abstract: This study investigated the synthesis of chitosan nanoascorbate (CSNA) using the ionotropic gelation method in the presence of a stabilizer, as well as the synthesis of CSNA from low-molecular-weight chitosan without a stabilizer. The physicochemical properties of the obtained CSNA samples were characterized using atomic force microscopy (AFM), Fourier-transform infrared (FTIR) spectroscopy, and dynamic light scattering (DLS). The CSNA samples derived from low-molecular-weight chitosan exhibited an average hydrodynamic diameter of 117 nm, whereas the samples synthesized from relatively high-molecular-weight chitosan by the ionotropic gelation method exhibited average hydrodynamic diameters of 360–380 nm. AFM analysis additionally revealed particles with lateral dimensions below 180 nm on the surface of the CSNA samples. The applicability of the nanostructured CSNA samples in sericulture was also evaluated. CSNA prepared from low-molecular-weight chitosan at an initial chitosan: ascorbic acid ratio of 4:1 and a concentration of 0.5% exhibited higher antimicrobial activity than both the initial components and the samples synthesized using the ionotropic gelation method.

Keywords: chitosan nanoascorbate from *Bombyx mori*, polymeric preparative form, degree of binding, nanoparticle size, FTIR spectroscopy.

Funding. This work was supported by the institutional budget of the Institute of Polymer Chemistry and Physics, Academy of Sciences of the Republic of Uzbekistan.

1. Introduction

Polycationic and polyanionic polysaccharides, which are the main components of marine algae, crustaceans, insects, and mulberry silkworm cocoons, can be considered as potential 1sources of immunomodulators. Chitosan (CS) is a non-toxic, biocompatible, and biodegradable polysaccharide exhibiting antimicrobial, antioxidant, anti-inflammatory, and immunostimulating activities, as well as other pharmacological properties. It promotes wound

healing, participates in tissue regeneration, and can serve as a carrier for the delivery of bioactive compounds, such as ascorbic acid (AA) [1–3]. It is well known that CS is insoluble in water but readily soluble in dilute organic acids; therefore, the preparation of water-soluble acidic derivatives of CS significantly expands its range of applications in agriculture [3]. CS derivatives with AA exhibit enhanced wound-healing, antimicrobial, and growth-stimulating properties compared with the parent components [4, 5]. A comparative analysis of the biological activity of CS nanoderivatives with organic acids has revealed increased interest in CS nanoderivatives with AA, since the resulting products are environmentally non-toxic and possess antimicrobial activity against plant and animal diseases [5, 6]. The investigation of the structural features of chitosan ascorbate nanoparticles remains a relevant research topic, since the interaction mechanisms between CS and AA strongly depend on the pH of the medium and temperature. According to the literature, the formation of chitosan–ascorbate systems can proceed via three principal interaction pathways. The first pathway involves the interaction between the enolic hydroxyl group at the C3 position (C3–OH) of AA and the amino groups of CS in aqueous media, resulting in the formation of a covalent donor–acceptor (coordination) complex at room temperature [7]. Under these conditions, the lactone ring of AA remains intact, while the amino groups of chitosan become protonated. The second pathway is associated with the interaction of the amino groups of CS with the enolic hydroxyl group at the C2 position (C2–OH) of AA, leading to the formation of imine (Schiff base) bonds in the presence of reducing agents such as sodium cyanoborohydride ($NaBH_3CN$) [8]. This process typically occurs at pH 5–6 and room temperature, where the more reactive enol groups of AA participate in bond formation. The third interaction pathway involves the thermal opening of the lactone ring of AA at elevated temperatures. At 60–70°C and pH 6–7, under an inert nitrogen atmosphere, the resulting carboxyl groups of AA react with the amino groups of CS to form covalent amide bonds, as confirmed by NMR spectroscopy [9, 10].

CS nanoparticles containing AA are commonly prepared via ionotropic gelation using sodium tripolyphosphate (STPP) as a cross-linking agent. In this system, nanoparticle formation occurs through electrostatic interactions between the positively charged protonated amino groups of CS and the negatively charged phosphate groups of STPP. The particle size is mainly influenced by the acid concentration and the degree of deacetylation (DD) of CS. CS with a higher DD possesses a greater number of free amino groups, resulting in a higher positive charge density and, consequently, a larger number of effective cross-linking sites with STPP [11]. Despite extensive studies on the biologically active properties of CS nanoderivatives, the literature lacks data on the application of CS nanoderivatives with AA in the field of sericulture

[3–5]. Most existing studies have focused on chitosan derivatives obtained from marine crustaceans, such as crabs and shrimps. In contrast, limited information is available on nanostructured chitosan–ascorbate complexes synthesized from chitosan derived from insect sources, particularly from the pupae of the mulberry silkworm, *Bombyx mori.*

In particular, there is a lack of systematic studies on the preparation of nanostructured chitosan–ascorbate systems based on both oligochitosan (OCS) and high-molecular-weight chitosan, as well as on the comparative evaluation of their antimicrobial properties and their potential application in sericulture. Therefore, in the present study, nanostructured chitosan–ascorbate complexes were synthesized using *Bombyx mori* chitosan and oligochitosan. Their antimicrobial properties were comparatively evaluated, and their effects on the growth and physiological parameters of the mulberry silkworm were assessed.

2. Materials and methods

CS was obtained from *B.M.* pupae through deproteinization, demineralization, and subsequent deacetylation in a 50 wt. % sodium hydroxide solution at 120 °C for 3 h in the pilot-scale facility of the Institute of Polymer Chemistry and Physics, Academy of Sciences of the Republic of Uzbekistan, following the procedure described in [1]. CS derived from *Bombyx mori* (*B.M.*) pupae, with a molecular weight of 123 kDa and a degree of deacetylation (DD) of 84 %, was used in this study. The DD of the initial CS samples was determined by conductometric titration in 0.1 N hydrochloric acid using a Mettler Toledo conductometer (USA). The molecular weight of the initial chitosan was determined by the viscometeric method using an Ubellode viscometer based on the Mark-Kuhn-Houwink equation [1].

High-Performance Size-Exclusion Chromatography (HP-SEC)

The weight-average (Mw) and number-average (Mn) molecular weights, as well as the polydispersity index (PDI), of oligochitosan and chitosan nanoascorbate (CSNA) derived from it were determined by high-performance size-exclusion chromatography (HP-SEC). The analyses were performed using an Agilent 1200 Series Chromatography system equipped with an isocratic pump, refractive index (RI) detector, and a PL-OH Mixed column. A buffer solution consisting of 0.3 M CH_3COOH/0.225 M CH_3COONH_4 (pH 4.5) was filtered through a 0.22 μm hydrophilic polyvinylidene fluoride (PVDF) Durapore membrane, degassed, and used as the mobile phase. The flow rate was 0.8 mL min^{-1}, while the column and detector temperatures were maintained at 25 °C. The injection volume was 50 μL, and the sample concentration was 0.001 g mL^{-1}. The HP-SEC system was calibrated using a series of monodisperse Pullulan standards (Fluka) with peak molecular weights (Mp) ranging from 1.08 to 710 kg mol^{-1}. The Mn, Mw, and PDI values were calculated from the resulting chromatograms.

2.1. Synthesis of CSNA (Chitosan Nanoascorbate) Samples.

Chitosan nanoascorbate (CSNA) was obtained by the ionotropic gelation method in an aqueous medium in the presence of a crosslinking agent, STPP, by varying the ratios of the initial components and the pH of the solution. The content of AA in the chitosan nanoascorbate (CSNA) was determined by alkaline titration using phenolphthalein as an indicator. The degree of AA binding was calculated based on the ratio (M_{AA})exp./(M_{AA})calc., as described in [12]. A 0.5% (w/v) aqueous solution of STPP (analytical grade) was used as a stabilizer and cross-linking agent. The resulting products were freeze-dried using an "Alpha Christ" lyophilizer (Germany) at −48°C for 5–6 h. The yield of the final products was evaluated as the ratio of the calculated mass to the experimentally obtained mass of the substance. The component ratios were calculated based on the molar concentrations of the starting materials.

To obtain chitosan nanoascorbate based on low-molecular-weight chitosan, acid hydrolysis of chitosan was carried out. The hydrolysis process was performed at a 1:1 (w/v) ratio of components in the presence of 1 M hydrochloric acid at a constant temperature of 75°C. The reaction time was 360 minutes. The reaction product was precipitated in the form of neutral (deprotonated) chitosan by adding an aqueous ammonia solution (NH_4OH), followed by washing with distilled water. The structure of the obtained oligochitosan sample was characterized by Fourier-transform infrared (FTIR) spectroscopy, while its molecular weight was determined by gel permeation chromatography (GPC) and dynamic light scattering (DLS).

Based on the obtained oligochitosan, further syntheses were carried out by controlling the ratio of the initial components and the pH of the reaction medium. Chitosan nanoascorbate (CSNA) was synthesized in an aqueous solution at a chitosan (CS) to ascorbic acid (AA) ratio of 2:1, without the use of sodium tripolyphosphate as a stabilizer. The synthesis time was 60 minutes, and the initial molar concentration of ascorbic acid in the aqueous solution was 0.05 mol/L. When the pH of the reaction system reached 5.92, the reaction product was precipitated using acetone and subsequently isolated.

The ascorbic acid content in the nanostructured chitosan–ascorbate sample obtained from oligochitosan was calculated based on the total nitrogen content determined by elemental analysis. Since multiple components are involved in the ionotropic gelation method, the degree of ascorbic acid binding was evaluated by determining the amount of free ascorbic acid through analytical titration.

The pH of the reaction system was measured at the end of the synthesis using a Bante 210 pH meter (China) at 25°C. Solutions of AA, titrant, and STPP were prepared using an analytical

method: the exact dry mass was weighed on an analytical balance, dissolved in distilled water, and thoroughly stirred on a stirrer until completely dissolved.

2.2. FTIR spectroscopy and AFM analysis

FTIR spectra were recorded using an Inventio-S FTIR spectrometer (Bruker, Germany) in the range of 500–4000 cm^{-1}. The size of CSNA nanoparticles was studied by atomic force microscopy (AFM) using an Agilent 5500 instrument (Agilent, USA). Silicon cantilevers with a stiffness of 9.5 $N•m^{-1}$ and a resonance frequency of 145 kHz were employed.

2.3. Dynamic Light Scattering (DLS) Analysis

Particle size determination was performed using dynamic light scattering (DLS) with a BeNano 90 nanoparticle size and zeta potential analyzer (Bettersize Instruments Ltd., China), equipped with a 671 nm solid-state laser. Measurements were performed at 25 °C using a 90° scattering angle. CSNA samples were dissolved in 2% (v/v) acetic acid at concentrations of 0.1%, 0.25%, and 0.5% at approximately 25 °C and allowed to dissolve completely for approximately 24 h. The pH of the resulting solutions was measured after complete dissolution.

Before measurement, the solutions were filtered through a microporous glass filter with a nominal pore size of 16 μm to remove large undissolved particles and prevent blockage of the measurement cell. Approximately 1 mL of each filtered sample was transferred into a PS cuvette for measurement. Each sample was measured five times, with 10 sub-runs per measurement. The laser intensity was automatically adjusted by the instrument according to the scattering properties of the sample.

The hydrodynamic diameter was determined from the autocorrelation function of the scattered-light intensity using the General analysis model implemented in the BeNano software.

For molecular-weight estimation, the hydrodynamic radius was related to the molecular weight using the Mark–Houwink-type relationship:

$$Rh = KM^{\alpha}$$

where Rh is the hydrodynamic radius, M is the molecular weight, K is the Mark–Houwink constant, and α is the Mark–Houwink exponent. The values $K=1.41\times10^{-4}$ and $\alpha=0.83$, reported for *Bombyx mori* chitosan, were used as reference parameters for molecular-weight estimation [5]. These parameters were not determined using external polymer standards during the DLS measurements. The same reference parameters were applied to the parent *Bombyx mori* chitosan and its nanoascorbate derivative because both samples were derived from the same chitosan source, thereby ensuring consistent conditions for comparative analysis. Therefore, the molecular-weight values obtained for the nanoascorbate samples were considered apparent (estimated) molecular-weight values rather than absolute molecular weights.

2.3. Analysis of CSNA by Atomic Force Microscopy (AFM).

The particle morphology and size of CSNA were analyzed by atomic force microscopy (AFM) using an Agilent 5500 AFM system (Agilent, USA). Imaging was performed in semi-contact (tapping/intermittent-contact) mode using silicon cantilevers with a stiffness of 9.5 N m^{-1} and a resonant frequency of 145 kHz. For sample preparation, diluted aqueous CSNA solutions were deposited onto a clean glass substrate and dried at room temperature prior to imaging.

2.4. Effect of the CSNA on the growth and development of mulberry silkworms

In these studies, solutions of samples synthesized by the ionotropic gelation method using initial component molar ratios of CS:AA:TPPNa = 4:1:0.5 were used. The effect of the CSNA on the growth and development of the mulberry silkworm was also evaluated under laboratory and field conditions. Field studies were conducted in Termez (Surkhandarya region) specialized enterprise “Inter Silk Pro.” Additional experiments were conducted in the laboratory “Mulberry Tree and Its Diseases and Pests” at the Research Institute of Sericulture. Silkworms of the “Uzbekistan-6” breed and their feed (mulberry leaves) were treated with a 0.025% solution of environmentally safe chitosan nanoascorbate (CSNA) and chitosan ascorbate (CSA).

The research materials included hybrid mulberry silkworm (*Bombyx mori*) eggs and larvae (Liang × Guang) imported from the People’s Republic of China for rearing during the summer–autumn season. In the experiments, polymer-based working solutions were tested, including chitosan (CS) and chitosan nanoascorbate (CSNA) containing 0.025% CSNA.

To evaluate the effects of the applied preparations during silkworm rearing, the number of dead and developmentally retarded larvae was continuously recorded. During the experiments, dead larvae or pupae were examined under a microscope, and diagnoses were made to identify the associated diseases. After completion of the silkworm rearing process, the following parameters were determined for both experimental and control groups: the number of normal, healthy, double, and black-spotted cocoons; the average weight of a single cocoon; cocoon shell weight; silk content; and cocoon yield obtained from 1 g of eggs.

2.5. Antimicrobial properties of the initial components and CSNA samples.

To evaluate the fungicidal activity of CSNA derived from oligochitosan and high-molecular-weight chitosan from *Bombyx mori*, the *Fusarium oxysporum* strain from the “Collection of Microorganisms with Industrial Significance” at the Institute of Microbiology, Academy of Sciences of Uzbekistan, was used as the test organism. Experiments were conducted in the “Synthesis of Advanced Polymers” laboratory at the Institute of Chemistry and Physics of Polymers, Academy of Sciences of Uzbekistan. The fungus was cultured under

sterile conditions and incubated on agar-based nutrient media. Fungicidal activity was assessed following the CLSI (Clinical and Laboratory Standards Institute) M100-30 standard using the uniform spore seeding method on the agar surface [13]. All experiments were performed in triplicate. To determine the antimicrobial properties of the initial components and CSNA samples, measurements were carried out in quadruplicate. The mean value (Mean) was calculated as:

$$\text{Mean} = \Sigma X / n \qquad (2),$$

where ΣX is the sum of all measured values and n is the number of measurements. The standard deviation (SD) was calculated using:

$$CO = \sqrt{\frac{(\Sigma\ (X - \text{Mean})^2}{(n-1)}} \qquad (3)$$

3 RESULTS AND DISCUSSION

3.1. Molecular Weight and Structural Properties of Chitosan Nanoascorbate Obtained on the Basis of Oligochitosan

After hydrolyzing the initial chitosan in a hydrochloric acid solution for 6 hours, a reduction in molecular weight was observed, reaching the 2–16 kDa range characteristic of oligochitosan. Following 6 hours of hydrolysis, the product yield was 40% relative to the initial chitosan. Upon completion of the hydrolysis, the product was precipitated using an aqueous ammonia solution and subsequently washed with distilled water. Based on the obtained low-molecular-weight oligochitosan, a CSNA sample (chitosan nanoascorbate) was synthesized. In the final product, the ratio of low-molecular-weight chitosan to ascorbic acid was determined by elemental analysis based on the nitrogen content. The nitrogen content of the starting chitosan was 8.36 %, while in the obtained chitosan nanoascorbate it was 6.18%. Calculations confirmed that the ascorbic acid content in the complex is 26%. The molecular weight properties of the obtained oligochitosan and the corresponding chitosan nanoascorbate (CSNA) samples are summarized in Table 1.

Table 1. Molecular weight properties of low-molecular-weight chitosan (oligochitosan) and the corresponding chitosan nanoascorbate

Sample names	Synthesis time (min)	Mn*10^3	Mw*10^3	Mz*10^3	PDI (Mw/Mn)
OCS	360	5,94	10,4	17,7	1,75
CSNA	-	7,68	14,8	26,3	1,93

For the low-molecular-weight chitosan samples, the Mn and Mw were determined. In addition, the average molecular weight (Mz) and the PDI were measured for all fractions. For

the low-molecular-weight chitosan, the weight-average and number-average molecular weights were found to be 10.4 kDa and 5.9 kDa, respectively, while the average molecular weight across all fractions was 17.7 kDa. For the chitosan nanoascorbate, the corresponding values were 14.8 kDa (Mw) and 7.68 kDa (Mn). The observed increase in the polydispersity index (PDI = Mw/Mn) of the synthesized chitosan nanoascorbate compared to the initial oligochitosan can be attributed to the redistribution of macromolecules during the synthesis process. The GPC chromatograms of the obtained samples are presented in Figure 1-2.

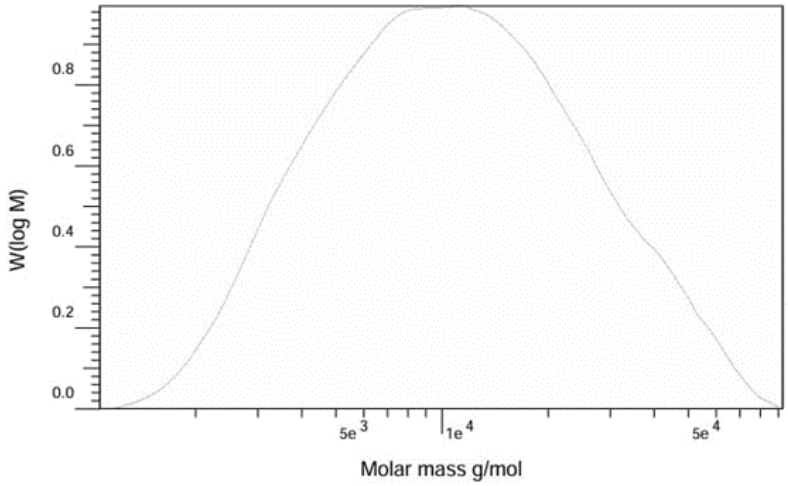


Fig. 1. GPC chromatograms of chitosan nanoascorbate samples derived from oligochitosan *Bombyx mori*

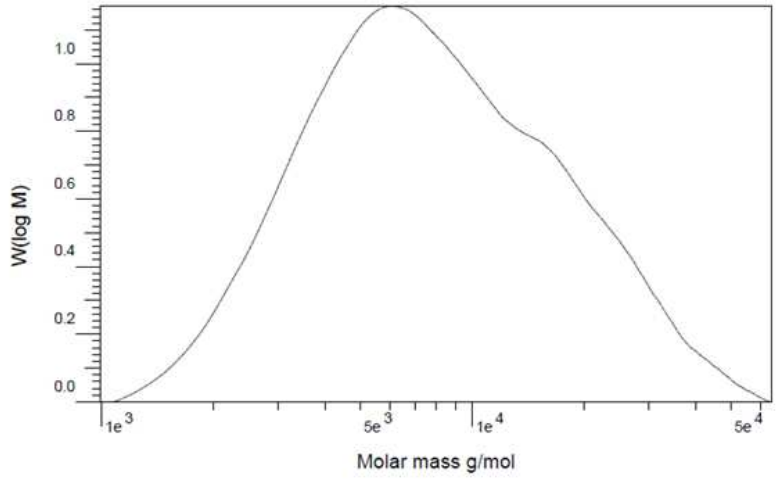


Fig. 2. GPC chromatograms of oligochitosan samples derived from *Bombyx mori*

The structure of the obtained olig chitosan samples and the chitosan nanoascorbate synthesized on their basis was confirmed by FTIR spectroscopy. For comparative analysis of the structural characteristics, FTIR spectra of the initial chitosans, oligochitosans, and their corresponding nanoascorbates were recorded. The obtained results are presented in Figure 3.

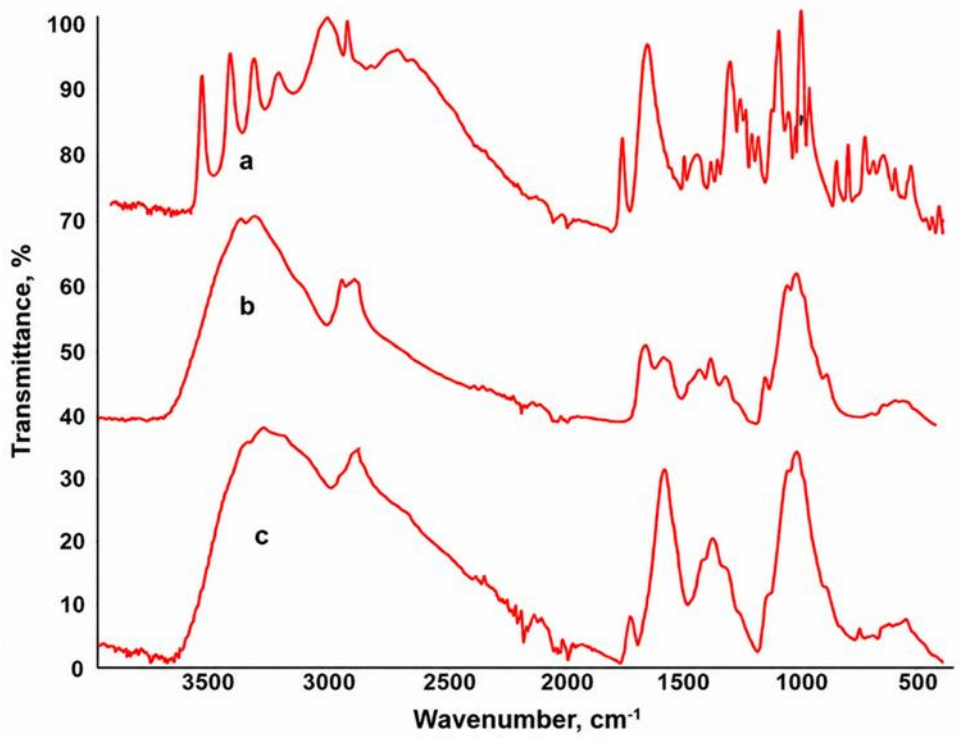


Fig. 3. FTIR spectra of ascorbic acid (a), oligochitosan (b), and chitosan nanoascorbate derived from *Bombyx mori* (c)

In the FTIR spectrum of chitosan (Fig. 3b), characteristic absorption bands were observed at 1645 and 1574 cm^{-1}, corresponding to the acetamide functional group (amide I) and amino groups, respectively. In the range of 1310–1420 cm^{-1} and at 2900 cm^{-1}, absorption bands attributable to methylene groups were detected. In the region of 3200–3350 cm^{-1}, broad absorption bands characteristic of hydroxyl groups were observed.

In the FTIR spectrum of ascorbic acid (Fig. 3a), absorption bands in the 3200–2900 cm^{-1} region correspond to the stretching vibrations of the C2 and C3 hydroxyl groups, while bands in the 2915–2900 cm^{-1} range are assigned to methylene groups. An absorption band at 1750 cm^{-1} is attributed to the carbonyl group within the lactone ring of ascorbic acid, and the band at 1650 cm^{-1} corresponds to C=C stretching vibrations. In addition, absorption bands at 1320, 1270, and 1140 cm^{-1} are characteristic of the C3, C2, and C5 hydroxyl groups.

In the FTIR spectrum of the obtained chitosan nanoascorbate (Fig. 3c), shifts in the characteristic absorption bands were observed compared with those of chitosan and ascorbic acid. A noticeable shift of the bands from 1645 and 1568 cm^{-1} toward lower wavenumbers was established, indicating the formation of chitosan nanoascorbate as a result of the interaction between the amino groups of the initial chitosan and the enolic group of ascorbic acid. In the 1400–900 cm^{-1} region, absorption bands characteristic of chitosan appeared with reduced intensity, suggesting a decrease in hydrogen bonding. The changes in intensity and the shifts of characteristic absorption bands in the FTIR spectrum of the ascorbate derived from low-

molecular-weight chitosan, compared with the spectra of the initial components—ascorbic acid and chitosan—confirm the formation of a water-soluble chitosan derivative, namely chitosan nanoascorbate.

Using dynamic light scattering (DLS) and *BetterSize* software, the average hydrodynamic diameter (Z-ave, d/nm), mean particle size (size, d/nm), particle size distribution, and molecular weight of the chitosan nanoascorbate synthesized from low-molecular-weight chitosan were determined. The DLS results indicate a bimodal distribution of the hydrodynamic radius (Rh) for the CSNA samples (Fig. 4).

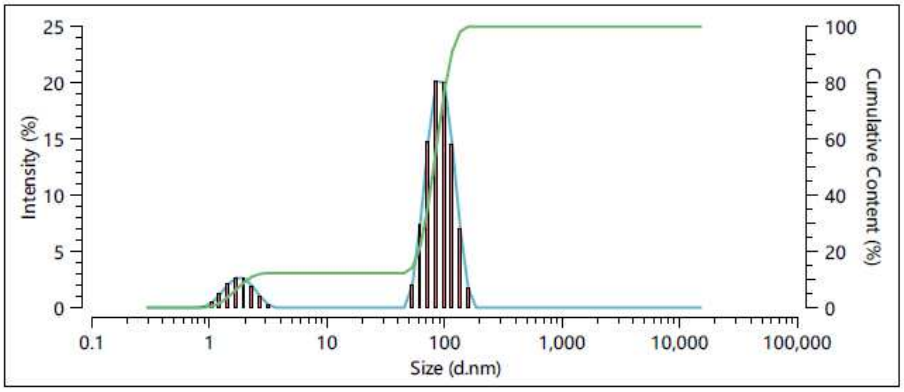
Results:

Z-ave (d.nm): 117.82 nm

Mw 6888.00 D

Intercept: 0.68

	Size (d.nm)	Area (%)	Std Dev (nm)	CV (%)
Peak 1	1.85	12.33	0.48	26.26
Peak 2	94.15	87.67	23.06	24.49
Peak 3				



Typical Values	Size (d.nm)
D10	2.13
D20	59.93
D30	67.90
D40	74.67
D50	80.79
D60	87.26
D70	94.45
D80	103.09
D90	114.69
D100	158.91

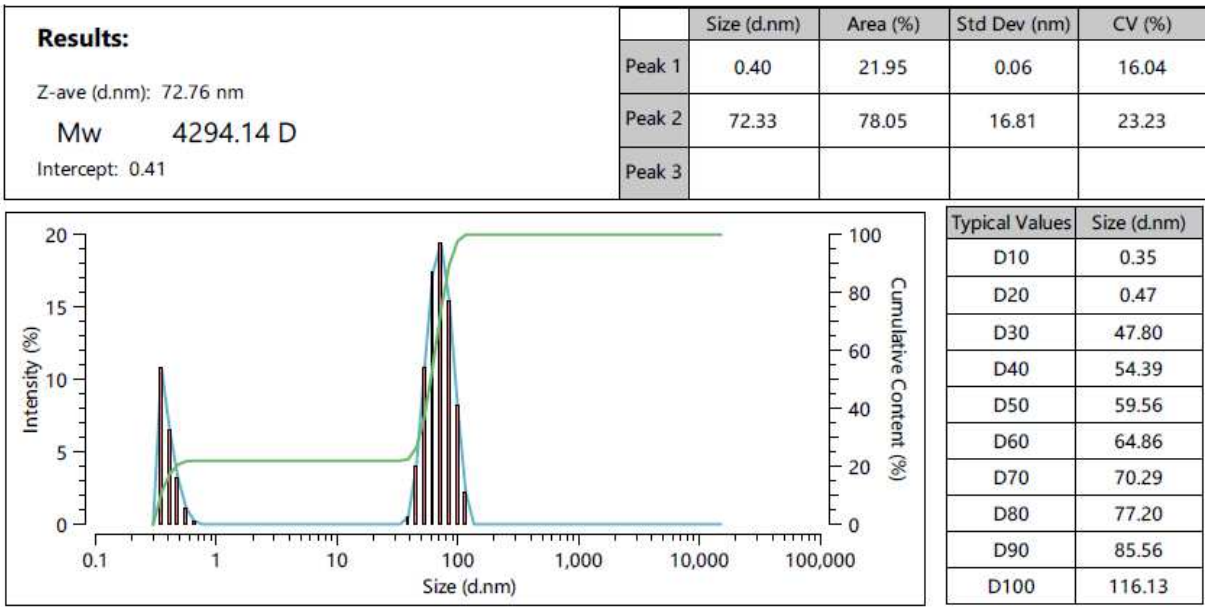
Fig. 4. Dynamic light scattering results of the CSNA solution

Two distinct populations were observed, with maxima at approximately Rh≈2 nm and Rh≈95 nm, corresponding predominantly to individual macromolecular particles of chitosan nanoascorbate and larger aggregated structures, respectively. The population with Rh≈2 nm predominated over the larger aggregates in both number- and mass-based distributions. Therefore, the DLS results were interpreted primarily based on the positions of the distribution maxima and the z-average hydrodynamic radius, rather than on the apparent boundaries of the size distribution, which cannot be determined precisely from the inverse reconstruction of the distribution from the measured correlation function.

The molecular-weight values estimated from the DLS measurements should be regarded as apparent molecular-weight estimates derived from the hydrodynamic size of the detected macromolecular species, rather than as direct measurements of the mass of individual macromolecules. The apparent molecular-weight value of 6.9 kDa was estimated from the z-average hydrodynamic diameter obtained by DLS (approximately 117 nm), using the empirical k and α constants established for *Bombyx mori* chitosan, as described in Section 2.3. Because

the CSNA sample exhibited a bimodal hydrodynamic-size distribution, the calculated value should be regarded as an apparent molecular-weight estimate based on the z-average hydrodynamic diameter of the sample rather than as the molecular weight of individual macromolecules. The obtained value is consistent with the oligomeric range reported for chitosan-based materials [14].

The DLS characteristics of CSNA were compared with those of the initial oligochitosan (OCS). The OCS sample exhibited a z-average hydrodynamic diameter of 72.76 nm, with the maximum of the intensity-weighted particle size distribution observed at approximately 72.33 nm, accounting for 78.05% of the total scattering intensity. The D50 value was 59.56 nm, corresponding to the 50% point of the cumulative distribution (Fig. 5).



	Size (d.nm)	Area (%)	Std Dev (nm)	CV (%)
Peak 1	0.40	21.95	0.06	16.04
Peak 2	72.33	78.05	16.81	23.23
Peak 3				

Typical Values	Size (d.nm)
D10	0.35
D20	0.47
D30	47.80
D40	54.39
D50	59.56
D60	64.86
D70	70.29
D80	77.20
D90	85.56
D100	116.13

Fig. 5. Dynamic light scattering results of the initial OCS solution

Following the formation of CSNA, the z-average hydrodynamic diameter increased to 117.82 nm, while the maximum of the intensity-weighted particle size distribution was observed at approximately 94.15 nm, accounting for 87.67% of the total scattering intensity. The D50 value also increased to 80.79 nm. The apparent molecular-weight values estimated from the DLS measurements were 4.29 kDa for OCS and 6.89 kDa for CSNA. These results show that formation of the CSNA complex is accompanied by an increase in the characteristic hydrodynamic size of the OCS-based system.

For comparison, the morphology of the CSNA-1 sample was examined by atomic force microscopy (AFM). The AFM images revealed numerous nanoscale surface features and individual objects with different lateral dimensions, including a substantial fraction of objects smaller than 50 nm. The observed lateral dimensions should not be directly compared with the hydrodynamic diameters obtained by DLS, since AFM and DLS characterize different physical

parameters. The height profile of the AFM image reached approximately 4 nm, providing complementary morphological information on the nanoscale organization of CSNA-1 (Fig. 6).

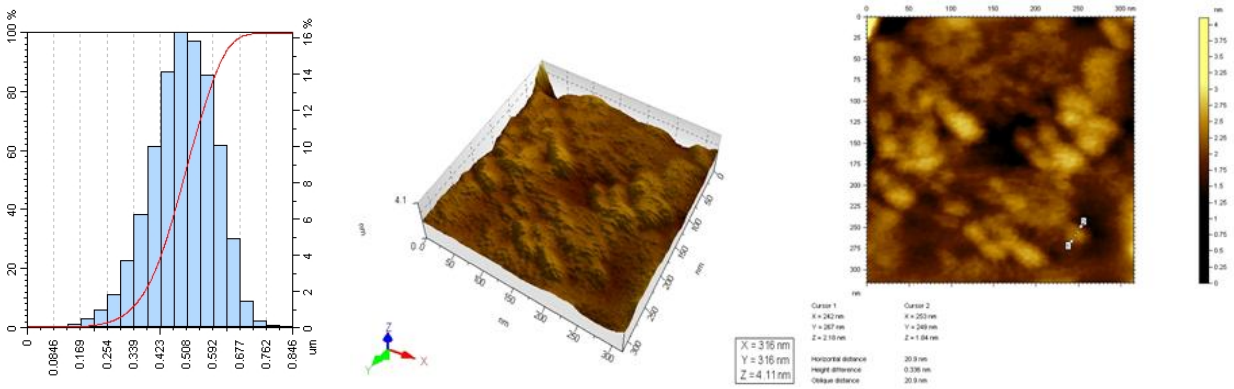


Fig. 6. AFM results of CSNA *B.M.*

In conclusion, chitosan nanoascorbate containing nanoscale structures was synthesized by controlling the component ratios using low-molecular-weight oligochitosan obtained through acid hydrolysis of high-molecular-weight chitosan. The molecular weights of the initial oligochitosan and the chitosan nanoascorbate were characterized by gel permeation chromatography (GPC), while DLS was used to evaluate their hydrodynamic size distributions. The DLS results revealed a bimodal distribution of hydrodynamic radius, with a predominant population of small macromolecular species and a second population corresponding to larger aggregates. AFM analysis provided complementary morphological evidence of nanoscale structures, including numerous objects with lateral dimensions below 50 nm.

3.2. Synthesis and structural properties of chitosan nanoascorbate from *Bombyx mori* using the ionotropic gelation method.

The influence of the ratio of the initial components CS, AA, and the stabilizer STPP on the properties of the resulting CSNA–AA complexes was investigated. It was established that an increase in the CS proportion leads to an increase in the solution pH and the yield of the final products, indicating enhanced interaction between CS and AA. Consequently, the amount of free AA in the reaction systems decreases. It was determined that a chitosan-to-ascorbic acid ratio of 4:1 is optimal, at which the yield of the final products reaches 82–87% [15, 16]. In addition, a 0.5 % aqueous solution of STPP used as a stabilizer was found to be optimal for the synthesis. In addition, the synthesis was found to be most efficient when using a 0.05 M AA solution. In the presence of the STPP stabilizer, the pH of the reaction system increases from 4.8 to 7.4. This occurs because, as the chitosan concentration in the system increases, the amount of free ascorbic acid decreases, while the reactivity of the initial chitosan is enhanced due to deprotonation of amino groups under near-neutral pH conditions. The obtained results are presented in Table 2.

Table 2. Dependence of the chitosan binding degree with ascorbic acid (t = 30 °C, τ = 60 min in the presence of STPP). The initial concentration of ascorbic acid was 0.05 mol/L

Component ratio CS : AA : STPP (mol/mol)	C_{AA}, ΔC mol/l	Binding degree, %	Yield, %
2:1:0,5	0,037	74,0	67,5
3:1:0,5	0,041	82,0	78,4
4:1:0,5	0,043	87,0	82,8
5:1:0,5	0,044	84,0	80,5

The highest degree of ascorbic acid binding and the maximum yield of the reaction product were observed at an initial component ratio of CS : AA : STPP = 4:1:0.5. Thus, at this ratio, the amino groups of chitosan achieve maximum saturation with ascorbic acid. It was found that further increasing the chitosan ratio has a negligible effect on the product yield.

The structural properties of the initial components—AA and CS—were investigated by FTIR spectroscopy. The obtained results showed that the FTIR spectra of CS exhibit characteristic absorption bands of amino and methylene groups at 1600 cm^{-1} and 1420 cm^{-1}, respectively, as well as a broad absorption band corresponding to hydroxyl groups in the 3000–3400 cm^{-1} region, which is in full agreement with literature data (Figure 7).

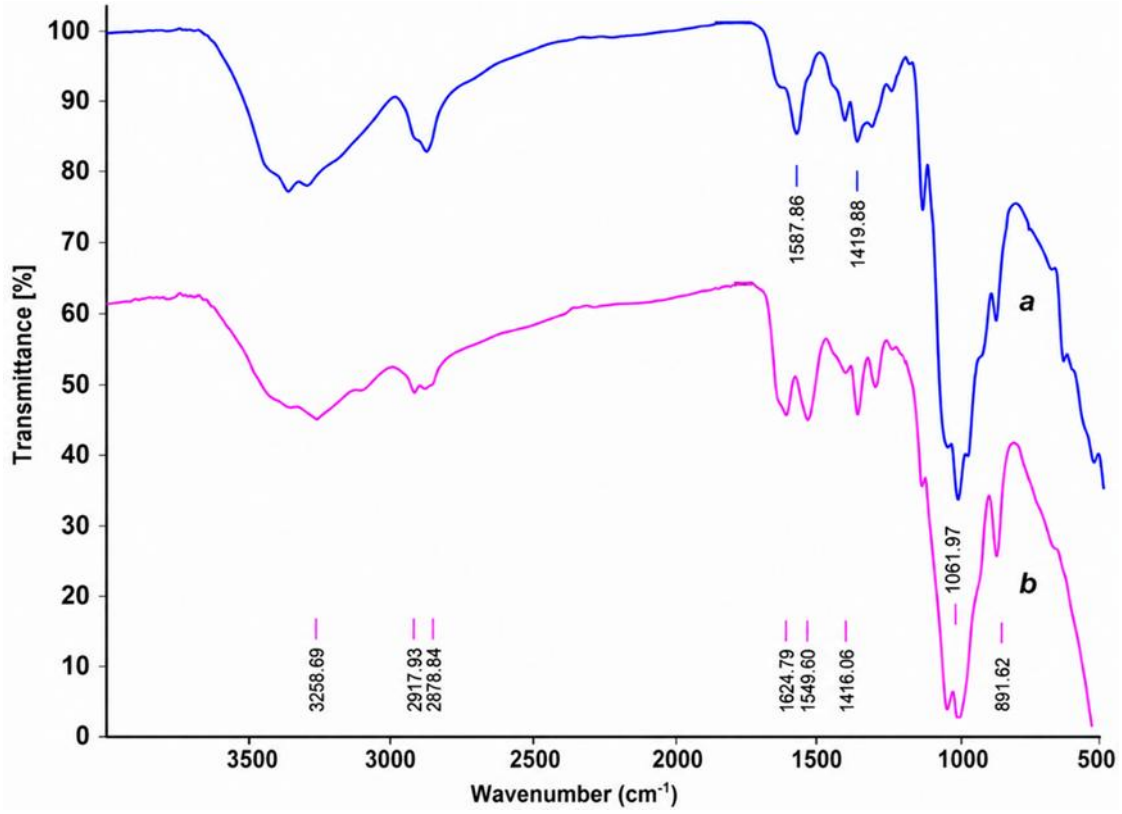


Fig. 7. FTIR spectra of *B.M.* CS (a) and *B.M.* CSNA (b)

In the FTIR spectra of AA, absorption bands attributed to hydroxyl groups were observed in the 3200–2900 cm^{-1} region, while bands corresponding to methylene groups appeared in the 2915–2900 cm^{-1} regions. In particular, absorption at 1750 cm^{-1} indicated the presence of carbonyl groups located in the lactone ring, whereas absorption around 1600 cm^{-1} was assigned to C=C double bonds of enolic groups [12].

In the FTIR spectra of the synthesized CSNA samples, a shift of the absorption band characteristic of CS amino groups from 1600 to 1540 cm^{-1} was observed, indicating the formation of a donor–acceptor interaction involving the amino groups of chitosan and the enolic group of AA. Additionally, newly appearing low-intensity absorption bands near 1796 cm^{-1} were identified as bands characteristic of lactone groups of AA.

AFM analysis of the CSNA samples obtained by the ionotropic gelation method revealed nanoscale structures with different lateral dimensions (Figs. 8 and 9).

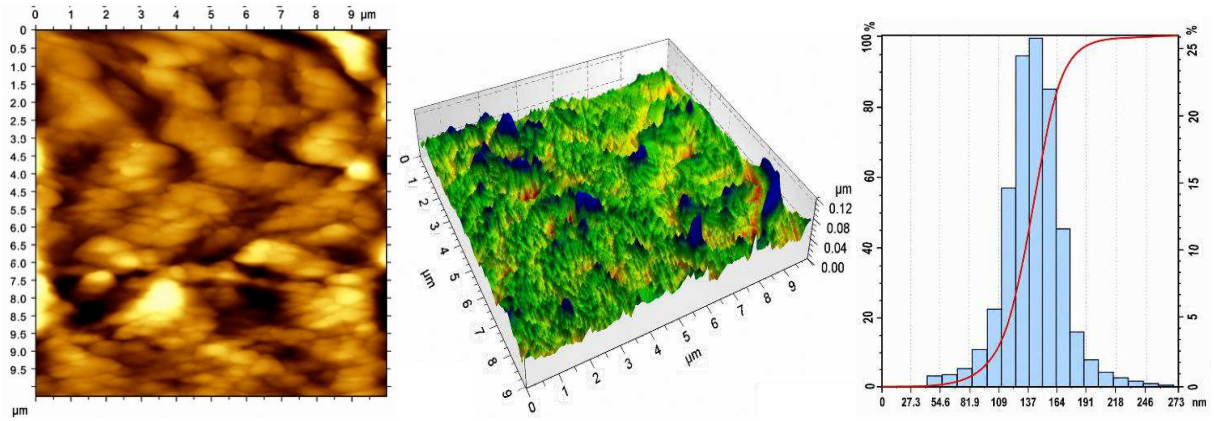


Fig. 8. Surface topography of chitosan nanoascorbate nanoparticles at a component ratio of 2:1:0.5

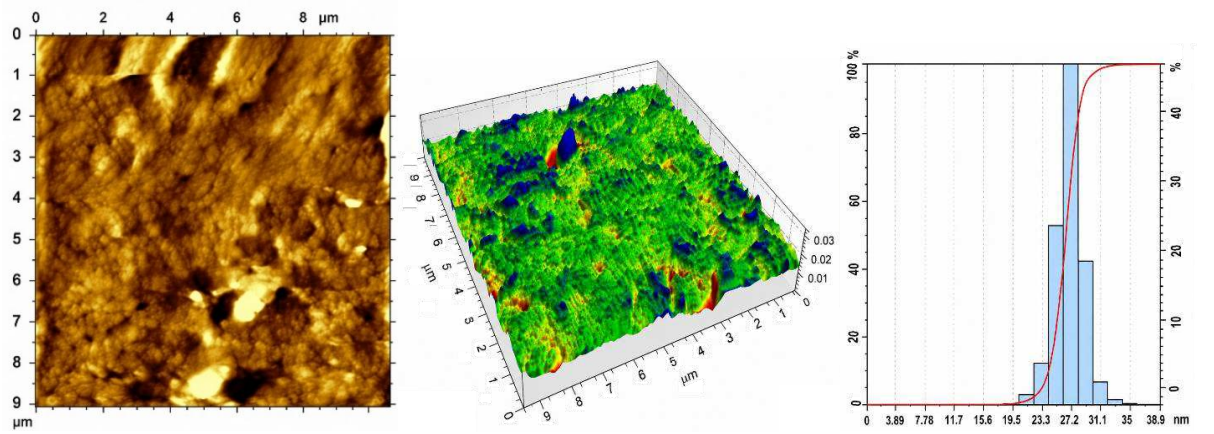


Fig. 9. Surface topography of chitosan nanoascorbate nanoparticles at a component ratio of 4:1:0.5

The size distributions obtained from the AFM images showed that the structures in Fig. 8 were predominantly in the range of approximately 80–180 nm, with a maximum around 130–150 nm, whereas the structures in Fig. 9 were mainly concentrated in the range of approximately 23–32 nm, with a maximum around 27–29 nm. The AFM height profiles reached approximately 120 nm and 30 nm for Figs. 8 and 9, respectively. These results indicate the presence of nanoscale and aggregated structures in CSNA and complement the hydrodynamic size data obtained by DLS.

For this purpose, the dynamic light scattering (DLS) method was employed using a BeNano 90 instrument. The molecular weight and particle size distribution of the CSNA solution with a component ratio of CS:AA:STPP = 4:1:0.25 were investigated, and the dependence of particle size on solution concentration was analysed. The DLS results showed that the CSNA particles exhibit a nanoscale size distribution, while their particle size remained relatively stable with increasing solution concentration. The DLS analysis showed an average hydrodynamic diameter (Z-average) of 567 nm. The intensity-weighted particle size distribution exhibited a maximum at approximately 379 nm, indicating that particles of this size make the greatest contribution to the measured intensity of scattered light. The D50 value of approximately 340 nm obtained from the cumulative distribution represents the particle size corresponding to 50% of the cumulative distribution and should not be interpreted as indicating that 50% of the particles have a diameter of 340 nm. Since the particle size distribution is weighted by scattering intensity, larger particles contribute disproportionately to the measured scattering intensity. The results are presented in Figure 10.

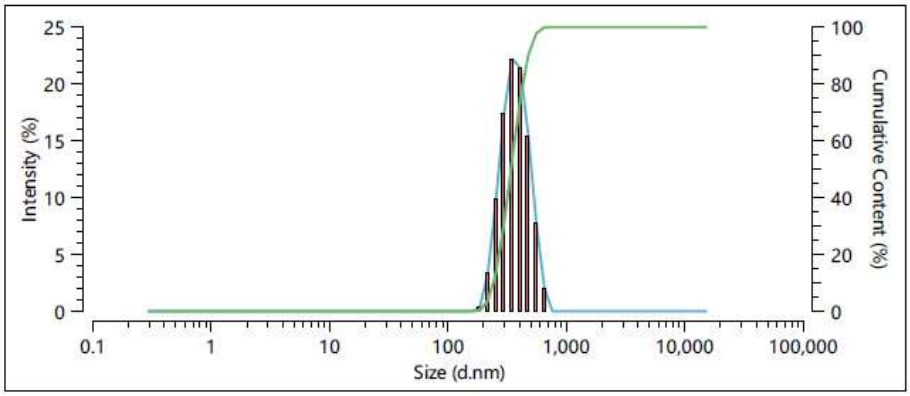
Results:

Z-ave (d.nm): 567.37 nm

Mw 119422.81 D

Intercept: 0.91

	Size (d.nm)	Area (%)	Std Dev (nm)	CV (%)
Peak 1	379.78	100.00	97.75	25.74
Peak 2				
Peak 3				



Typical Values	Size (d.nm)
D10	240.61
D20	270.03
D30	294.78
D40	317.74
D50	340.47
D60	366.43
D70	394.02
D80	430.58
D90	475.29
D100	651.73

Fig. 10. Results of DLS analysis: particle size distribution and molecular weight of a 0.5 % CSNA solution

Upon dilution of the CSNA solution from 0.5% to 0.25%, the average hydrodynamic diameter was 578 nm, while the maximum of the intensity-weighted particle size distribution was observed at approximately 360 nm. These values are close to those obtained for the initial 0.5% CSNA solution, indicating that dilution within this concentration range does not result in substantial changes in the particle size distribution. The relatively small variation in the hydrodynamic diameter and the position of the distribution maximum indicates that the hydrodynamic characteristics of the CSNA particles remain stable upon dilution from 0.5% to 0.25% (Figure 11).

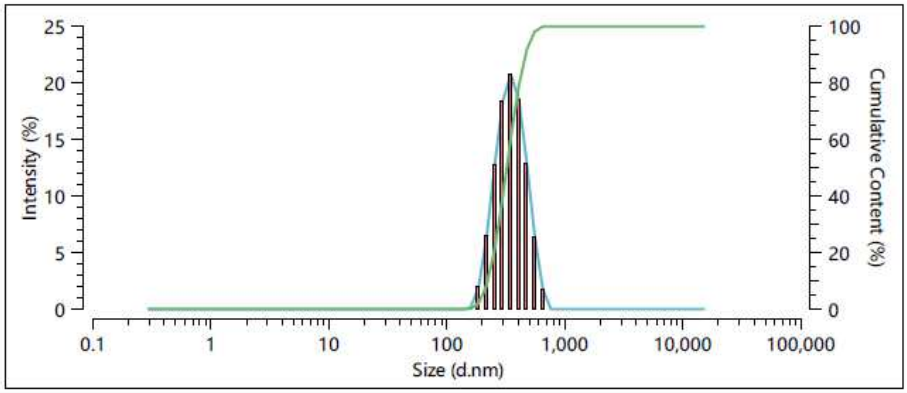
Results:

Z-ave (d.nm): 578.39 nm

Mw 122222.13 D

Intercept: 0.98

	Size (d.nm)	Area (%)	Std Dev (nm)	CV (%)
Peak 1	360.86	100.00	101.14	28.03
Peak 2				
Peak 3				



Typical Values	Size (d.nm)
D10	221.55
D20	250.48
D30	274.68
D40	298.16
D50	322.50
D60	346.84
D70	378.30
D80	412.17
D90	465.91
D100	651.73

Fig. 11. Results of DLS analysis: particle size distribution and molecular weight of a 0.25 % CSNA solution

However, a decrease in the CSNA solution concentration was accompanied by a gradual shift of the maximum of the intensity-weighted particle size distribution toward smaller particle sizes. At a concentration of 0.5%, the maximum was observed at approximately 379 nm, decreasing to approximately 360 nm at 0.25% and 327 nm at 0.1%. This behavior indicates a slight reduction in the fraction of relatively larger particles upon significant dilution. Comparison of the 0.5% and 0.1% CSNA solutions shows that the average molecular weight and mean hydrodynamic particle size remain essentially stable, while the maximum peak value decreases. This trend can be attributed to a relative decrease in the proportion of larger particles as the solution concentration decreases.

3.3. Evaluation of the effectiveness of CSNA on the growth and productivity of silkworms.

Mulberry leaves used as feed were treated three times with CSNA and then fed to silkworms of the “Monovoltin” variety. As a result, cocoon yield increased on average by 8-

10% compared to the control group (in which mulberry leaves were washed with water only). The treatment also contributed to enhanced viability and productivity of the silkworms.

To evaluate the effect of the treatment during feeding, the average number of cocoons obtained in each experimental variant was recorded, their average weight was determined, and the results were compared with those of the control group. The experiments were conducted in triplicate using silkworms of the "Uzbekistan-6" variety. The obtained results are presented in Table 3.

Table 3. Cocoon yield of silkworms of the "Uzbekistan-6" variety treated with chitosan ascorbate (CSA) and CSNA (initial number of larvae: 200).

№	Treatments	Number of healthy cocoons (units)	Average number of formed cocoons (no.)	Number of unformed cocoons (no.)	Viability (%)	Average mass of 1 cocoon (g)		Cocoon mass (g)	Average mass (g)
1	Control	166	168	5	83.0	1.80	1.66	299.0	279.0
		173		4	86.5	1.60		278.0	
		165		9	82.5	1.58		260.0	
2	CSA 0.025 %	166	174	6	83.0	1.55	1.65	258.0	287.0
		165		8	82.5	1.70		279.0	
		190		5	95.0	1.70		323.0	
3	CSNA 0.025 %	181	174	6	90.5	1.63	1.75	295.0	297.0
		162		4	81.0	1.78		288.0	
		179		9	83.5	1.84		308.0	

As shown in the table, the average number of formed cocoons following treatment with CSA and CSNA was 3.5% higher than the control. The average cocoon mass under CSNA treatment exceeded the control by 5.15%. Examination of the mass of formed cocoons demonstrated that treatment of silkworm feed with CSA and CSNA resulted in an increase in the average cocoon mass of up to 6.5 % compared to the control.

For the experimental studies, working solutions of CS and CSNA were prepared. Silkworm larvae hatched from hybrid eggs imported from the People's Republic of China were used in the experiments. An experimental design was developed to evaluate the effects of these preparations at different concentrations.

To prevent any adverse effects on the silkworms, beginning from the fourth instar, the tested preparation solutions were applied twice daily (morning and evening) by spraying them onto the mulberry leaves used as feed (Figure 12).



Fig. 12. Silkworms reared with CSNA (a) and CS (b) preparations, and the cocoon yield obtained under CSNA treatment

The experiment was conducted according to the following regimen:

On the first day of the fourth instar, nuclear polyhedrosis disease was induced by cold stress. From the second day of the fourth instar until the onset of molting, silkworms were treated with the preparations for 4 days. From the first day of the fifth instar until cocoon spinning, the silkworms were fed with the preparations for 7–9 days. During the experiments, key biological parameters of the silkworms were evaluated, including larval viability, the number of normal cocoons, and the average weight of a single cocoon. The results obtained for the experimental and control groups are presented in Table 4.

Table 4. Biological parameters of silkworms (summer 2025)

Variants	Larval viability, $\overline{X} \pm S_{\overline{x}}$, %	Disease incidence, $\overline{X} \pm S_{\overline{x}}$, %	Larval mortality, $\overline{X} \pm S_{\overline{x}}$, %	Larval period duration, days
Chinese hybrid silkworm strain "Liang × Guang"				
CSNA	84,0±0,8	4,45±0,90	5,5±1,1	27
CS	80,5±1,45	8,10±0,52	7,0±1,1	28
Control	78,5±1,10	8,89±0,74	8,0±0,8	30

Analysis of the data presented in Table 4 shows that all experimental variants outperformed the control. Larval viability in the CSNA and CS treatments ranged from 80.5 to 84.0%, whereas in the control it was 78.5%, corresponding to an increase of 2.0–5.5%. Disease incidence in the experimental variants ranged from 4.45 to 8.1%, compared with 8.89 % in the control. Thus, feeding with the tested preparations resulted in a reduction in disease incidence of 0.79% for CS and 4.44% for CSNA.

Furthermore, the proportion of larvae that exhibited delayed development or died due to nuclear polyhedrosis disease decreased to 5.5% in the experimental groups, compared with 8.0% in the control, representing a reduction of 2.1–2.5 percentage points.

3.4. Antimicrobial properties of CSNA.

The effect of chitosan nanoderivatives derived from *Bombyx mori* and synthesized in the presence of ascorbic acid on the growth of the fungal culture *Fusarium oxysporum* was investigated. The obtained results confirm the presence of moderate antimicrobial activity in the solutions of the initial components, namely chitosan and ascorbic acid. In addition, it was established that chitosan nanoderivatives synthesized in the presence of ascorbic acid at a component ratio of chitosan : organic acid : sodium tripolyphosphate (4:1:0.5) exhibit higher antimicrobial activity compared to other nanoderivatives prepared at different component ratios. The obtained data are presented in Table 5.

Table 5. Effect of chitosan nanoascorbate and the initial components on the fungus *Fusarium oxysporum*

№	Variants	Cross-sectional diameter (mm)	Number of replicates			Total zone diameter (mm) (mean ± SD) 72 h.
			I	II	III	
1	Acetic acid - 2 %	10	35	21	10	22±5
2	CS -0,5%	10	25	22	20	22,3 ± 2,5
3	AA-0,5	10	18	12	13	14,2 ± 2.63
4	CSNA 2:1:0,5-0,5%	10	20	26	28	24,6 ± 4.6
5	CSNA 4:1:0,5-0,5%	10	24	25	29	26 ± 2
6	CSNA (4:1) prepared from LMW CS	10	35	35	33	34,0±1

It should be noted that a 0.5% CSNA solution from *Bombyx mori* formed an inhibition zone with a diameter of 26 ± 2 mm, exhibiting relatively high fungicidal activity. To enhance its antimicrobial properties, chitosan nanoascorbate from Bombyx mori was synthesized using low-molecular-weight chitosan by varying the ratio of the initial components. The results indicated that, at a component ratio of low-molecular-weight chitosan to ascorbic acid of 4:1,

the chitosan nanoascorbate produced the largest inhibition zone against the growth of Fusarium oxysporum (34.0 ± 1 mm) compared with the initial chitosan and corresponding acids.

4. Conclusions

CSNA was successfully synthesized from *Bombyx mori* chitosan using both ionotropic gelation in the presence of a stabilizer and low-molecular-weight chitosan in the absence of a stabilizer. The synthesized CSNA samples were characterized by FTIR spectroscopy, AFM, and DLS, confirming their distinct structural and nanoscale characteristics.

AFM analysis of the low-molecular-weight chitosan-derived CSNA revealed numerous nanoscale structures, including a substantial fraction of objects smaller than 50 nm, with a maximum height of approximately 4 nm. For the ionotropic-gelation-derived CSNA samples, the AFM analysis revealed nanoscale structures with characteristic lateral dimensions centered at approximately 130–150 nm and 27–29 nm, with corresponding height profiles of approximately 120 and 30 nm, respectively. These AFM observations provide complementary morphological evidence for the nanoscale organization of CSNA.

Comparison of the DLS characteristics of the initial OCS and CSNA showed an increase in the characteristic hydrodynamic size following formation of the nanoascorbate complex. The z-average hydrodynamic diameter increased from 72.76 nm for OCS to 117.82 nm for CSNA, while the maximum of the intensity-weighted particle size distribution shifted from approximately 72.33 to 94.15 nm. These results indicate a change in the hydrodynamic characteristics of the OCS-based system upon CSNA formation.

The biological evaluation demonstrated antifungal activity of CSNA against Fusarium oxysporum. Among the tested samples, CSNA prepared from low-molecular-weight chitosan at an initial CS:AA ratio of 4:1 exhibited the highest inhibition zone of 34.0 ± 1.0 mm.

Application of CSNA in silkworm rearing resulted in a slight increase in cocoon yield compared with the control and was associated with a reduction in the number of unformed cocoons.

Declarations

Ethics approval and consent to participate. *Not applicable.*

Consent for publication. *Not applicable.*

Availability of data and materials. *No specialized software, databases, or external datasets were used in this study. The data generated and analyzed during the current study are available from the corresponding author upon reasonable request.*

Competing interests. *The authors declare that they have no competing interests.*

Authors' contributions. *Pirniyazov Kudrat Kadambayevich: Writing – original draft, formal analysis, investigation, methodology; Rashidova Sayyora Sharafovna: Conceptualization, supervision, writing – review and editing.*

Acknowledgments. *The authors express their gratitude to the staff of the Laboratory of Physical and Physicochemical Analysis, Institute of Polymer Chemistry and Physics, Academy of Sciences of the Republic of Uzbekistan, for carrying out the physicochemical studies.*

References

[1] Rashidova SSh, Milusheva RYu (2009) Chitin and chitosan from *Bombyx mori*: Synthesis, properties and applications. Fan, Tashkent.

[2] Sekar V, Rajendran K, Vallinayagam S, Deepak V, Mahadevan S (2018) Synthesis and characterization of chitosan ascorbate nanoparticles for therapeutic inhibition for cervical cancer and their in silico modeling. Journal of Industrial and Engineering Chemistry. 62: 239-249. https://doi.org/10.1016/j.jiec.2018.01.001

[3] Pirniyazov KK, Rashidova SSh (2020) Synthesis of ascorbate and nanoascorbate of chitosan and their biologically active properties. Science and Innovative Development. 5: 47–62..

[4] Mawazi SM, Kumar M, Ahmad N, Ge Y, Mahmood S (2024) Recent Applications of Chitosan and Its Derivatives in Antibacterial, Anticancer, Wound Healing, and Tissue Engineering Fields. Polymers, 16(10), 1351. https://doi.org/10.3390/polym1610135

[5] Pirniyazov KK, Asrakulova DI, Rashidova SSh (2024) Synthesis and antimicrobial properties of chitosan nanoascorbate of *Bombyx mori*. Moscow University Chemistry Bulletin. 79 (5), 345–350. https://doi.org/10.3103/S002713142470038X.

[6] Iskandarov TI, Romanova LKh et al. (2021) The first toxicological passport for the nanoascorchit preparation. Ministry of Health of the Republic of Uzbekistan, Tashkent.

[7] Liping L, Kexin L, Huipu D, Jia L, Jie Z (2020) Study on Preparation of a Chitosan/Vitamin C Complex and Its Properties in Cosmetics. Natural Product Communications. 15: 1–9. https://doi.org/10.1177/1934578X20946876

[8] Hafsa J, Charfeddine B, Smach MA, Limem K, Majdoub H, Sonia R (2014) Synthesis, characterization, antioxidant and antibacterial proprieties of chitosan ascorbate. International Journal of Pharmaceutical and Chemical Sciences. 4: 1072–1081.

[9] Zhuang L, Zhi X, Du B, Yuan S (2020) Preparation of Elastic and Antibacterial Chitosan–Citric Membranes with High Oxygen Barrier Ability by in Situ Cross-Linking. ACS Omega. 5: 1086–1097 https://doi.org/10.1021/acsomega.9b03206

[10] Yalinca Z, Yilmaz E, Taneri B, Bullici F, Tuzmen SJ (2013) Blood Contact Properties of Ascorbyl Chitosan. Journal of Biomaterials Science, Polymer Edition. 24, 1969–1987. https://doi.org/10.1080/09205063.2013.816929

[11] Othman N, Masarudin MJ, Kuen CY Dasuan NA Abdullah LC Jamil Md SNA (2018) Synthesis and Optimization of Chitosan Nanoparticles Loaded with L-Ascorbic Acid and Thymoquinone. Nanomaterials. 8, 920. https://doi.org/10.3390/nano8110920

[12] Pirniyazov KK, Rashidova SSh (2020) Study of the Kinetics of *Bombyx mori* Chitosan Ascorbate Formation. Bulletin of the Karaganda University CHEMISTRY series. 3(99): 38-43. https://doi.org/10.31489/2020Ch3/38-43

[13] CLSI. (2020) Performance Standards for Antimicrobial Susceptibility Testing: 30th Ed. CLSI document M100. – Wayne, P.A.: Clinical and Laboratory Standards Institute. P. 296.

[14] Blagodatskikh IV, Kulikov SN, Vyshivannaya OV, Bezrodnykh EA and Tikhonov VE (2017) N-Reacetylated Oligochitosan: pH Dependence of Self-Assembly Properties and Antibacterial Activity. Biomacromolecules. 18(5): 1491–1498. https://doi.org/10.1021/acs.biomac.7b00039

[15] Sreekumar S, Goycoolea FM, Moerschbacher BM, Rivera-Rodriguez GR (2018) Parameters influencing the size of chitosan-TPP nano- and microparticles. Sci. Rep. 8: 4695. https://doi.org/10.1038/s41598-018-23064-4

[16] Pirniyazov KK, Rashidova SSh (2025) Comparative properties of chitosan hydrochloride and chitosan nanoacetate from *Bombyx mori*. UJP. 4(3): 25-36.